International Journal of Biological Macromolecules 137 (2019) 261–269

Contents lists available at ScienceDirect

International Journal of Biological Macromolecules

journal homepage: http://www.elsevier.com/locate/ijbiomac

Discovery of a highly specific and efficacious inhibitor of human carboxylesterase 2 by large-scale screening

Yun-Qing Song [a,1], Xiao-Qing Guan [a,1], Zi-Miao Weng [a,b,1], Ya-Qiao Wang [a], Jing Chen [c], Qiang Jin [a], Sheng-Quan Fang [b], Bin Fan [b], Yun-Feng Cao [d], Jie Hou [b,*], Guang-Bo Ge [a,*]

[a] Translational Medicine Center, Yueyang Hospital of Integrated Traditional Chinese and Western Medicine & Institute of Interdisciplinary Integrative Medicine Research, Shanghai University of Traditional Chinese Medicine, Shanghai 200473, China
[b] Department of Biotechnology, College of Basic Medical Sciences, Dalian Medical University, Dalian 116044, China
[c] School of Life Science and Medicine, Dalian University of Technology, Panjin 124221, China
[d] Key Laboratory of Contraceptives and Devices Research, Shanghai Engineering Research Center of Reproductive Health Drug and Devices, Shanghai Institute of Planned Parenthood Research, Shanghai 200032, China

ARTICLE INFO

Article history:
Received 28 May 2019
Received in revised form 27 June 2019
Accepted 28 June 2019
Available online 29 June 2019

Keywords:
Glabridin
Human carboxylesterase 2 (CES2A)
Specific inhibitor
Inhibition mechanism
Irinotecan-induced diarrhea

ABSTRACT

Human carboxylesterase 2 (CES2A), one of the most abundant hydrolases distributed in human small intestine and colon, play key roles in the hydrolysis of a wide range of prodrugs and other esters. Recent studies have demonstrated that CES2A inhibitors may ameliorate irinotecan-induced severe diarrhea, but the specific and efficacious inhibitors targeting intracellular CES2A are rarely reported. Herein, a large-scale screening campaign was conducted for discovery of potent and specific CES2A inhibitor(s). Following screening of more than one hundred of natural products, glabridin (a bioactive compound of *Glycyrrhiza glabra* L.) was found displaying potent inhibition on CES2A and high specificity over CES1A (>500-fold) and other serine hydrolases. Further investigation showed that glabridin was cell permeable and low cytotoxic, as well as capable of inhibiting intracellular CES2A in living cells, with the IC_{50} value of 0.52 μM. Molecular dynamics simulations showed that glabridin formed strong and stable interactions with both the catalytic cavity and Z site of CES2A *via* hydrophobic interactions. In summary, glabridin was a potent and specific inhibitor targeting intracellular CES2A, which could be used as an ideal lead compound to develop more efficacious CES2A inhibitors for modulating the pharmacokinetic behaviors of CES2A-substrate drugs and alleviating irinotecan-induced diarrhea.

1. Introduction

Mammalian carboxylesterases (CEs, EC. 3.1.1.1) are key serine hydrolases in mammals, which are localized in the lumen of the endoplasmic reticulum and responsible for the hydrolytic metabolism of a wide range of compounds that bearing of ester and amide bonds [1,2]. In the human body, CES1A or CES2A are two predominant CES isoenzymes that have been extensively studied over the twenty years. Generally, CES1A is abundantly distributed in hepatocytes and adipocytes, and prefers to hydrolyze the ester/amide substrates that bearing a bulky acyl group and a small alcoholic unit (such asoseltamivir, clopidogrel and enalapril) [3,4]. In addition to xenobiotic metabolism, CES1A also participates in the hydrolysis of some key endogenous esters (such as cholesteryl esters), and has been considered as a therapeutic target to regulate cholesterol homeostasis and lipid metabolism [5,6]. By contrast, CES2A is abundantly distributed in the small intestine and colon, while this enzyme prefers to hydrolyze the ester/amide substrates with a relatively large alcohol/amine group and a small acyl group, such as irinotecan, capecitabine, tenofovir disoproxil and flutamide [3,4,7–9]. Although recent studies demonstrate that CES2A displays triacylglycerol (TG) hydrolytic activity [10], the predominant biological roles of this enzyme seems the hydrolytic metabolism of ester-containing xenobiotics and the activation of prodrugs (such as irinotecan, tenofovir disoproxil, capecitabine and LY2334737, the prodrug of gemcitabine) [3,4,11,12].

Among all reported CES2A substrate drugs, irinotecan (also called CPT-11) has drawn much attention from pharmacologists, toxicologists and clinical research specialists, due to the severe intestinal toxicity triggered by this anticancer agent [13]. Following the intravenous injection administration of irinotecan, this agent can be slowly converted into its active metabolite SN-38 by hepatic CES, while SN38 could be readily metabolized to form its inactive O-glucuronide (SN-38G) by hepatic UDP-glucuronosyltransferases [14]. Irinotecan and its metabolites (including SN-38 and SN-38G) can be transported into the intestinal tract *via* the efflux transporters expressed in the bile duct [15]. Once transported into the intestinal tract, irinotecan can be hydrolyzed to

* Corresponding authors.
E-mail addresses: houjie@dlmedu.edu.cn (J. Hou), geguangbo@dicp.ac.cn (G.-B. Ge).
[1] These authors contributed equally to this work.

https://doi.org/10.1016/j.ijbiomac.2019.06.235
0141-8130/

SN-38 by intestinal CES2A, while SN-38G can be deconjugated by bacterial β-glucuronidase to SN-38 [16]. Both processes lead to the over-accumulation of SN-38 (a potent cytotoxic agent for the intestinal epithelial cells) in the intestinal tract, and thereby trigger severe delayed diarrhea [13]. Therefore, co-administration with selective and more efficacious CES2A inhibitors may ameliorate irinotecan induced life-threatening diarrhea for the patients receiving irinotecan, thereby improving the patient's quality of life [17].

Over the past two decades, a wide range of CES2A inhibitors with chemically diverse scaffolds (such as flavonoids, triterpenoids, tanshinones, benzene sulfonamides and trifluoroketones) have been reported [18–20], which encouraged the medicinal chemists to develop more efficacious CES2A inhibitors with excellent specificity and high safety profile, for modulation of irinotecan intestinal toxicity. Although numerous CES2A inhibitors including natural products and synthetic compounds have been reported, the potent and highly specific CES2A inhibitors that capable of inhibiting intracellular CES2A are rarely reported [21]. Ideal orally administrated CES2A inhibitors for modulation of irinotecan intestinal toxicity should meet the following three requirements, 1) potent and highly specific; 2) cell-permeable and capable of targeting intracellular CES2A; 3) high intestinal exposure but low exposure to other organs, such as the liver. Currently, loperamide (a specific CES2A inhibitor) has been used for the prevention and treatment of irinotecan induced delayed onset diarrhea in clinic, but the moderate inhibition potency and the side-effects of loperamide (such as constipation, drowsiness, lethargy, and nausea) strongly limits the clinical applications of this agent [22]. Thus, it is necessary to develop more efficacious and highly specific CES2A inhibitors with improved pharmacokinetic properties to modulate the treatment outcomes of irinotecan, which may provide alternative chemotherapeutic agents for ameliorating irinotecan induced severe diarrhea.

This study aimed to find ideal lead compound(s) for the development of highly specific inhibitors of CES2A over other human serine hydrolases. To this end, more than one hundred of natural compounds were collected and a high-throughput screening campaign was carried out using a panel of fluorescence-based biochemical assays. Following large-scale screening, glabridin (Fig. 1), one of the major bioactive constituents in the roots of *Glycyrrhiza glabra* L. [23], was found with excellent CES2A inhibition activity and high specificity over CES1A. Such finding encouraged us to further investigate the specificity of glabridin over other human serine hydrolases, as well as to characterize the inhibition behaviors and mechanism of action of this natural compound. Meanwhile, the inhibition potential of glabridin targeting intracellular CES2A was also investigated in living cells. Furthermore, molecular dynamics simulations were performed to investigate the key interactions between glabridin and CES2A, as well as to gain mechanistic insights into the inhibition of glabridin on CES2A from the viewpoint of enzyme-ligand interactions. All these studies would be very helpful for the discovery and development of more efficacious CES2A inhibitors with improved properties.

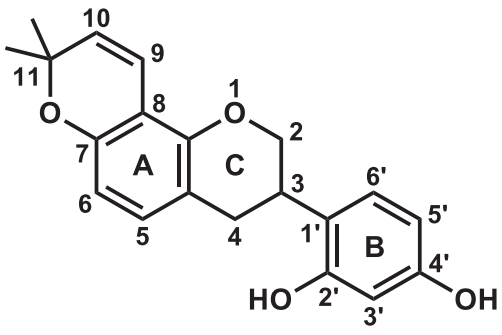

Fig. 1. The chemical structure of glabridin.

2. Materials and methods

2.1. Chemicals and materials

In the present study, a total of 112 natural compounds including glabridin were obtained from Chengdu Pufei Biotech Co., Ltd. (Chengdu, China). The origin of fluorescein diacetate (FD), D-luciferin methyl ester (DME), loperamide (LPA), Oleanolic acid (OA) and Luciferin Detection Reagent (LDR) was reported in a previous study [24]. Phenacetin, irinotecan and SN38 were obtained from Tianjin Heowns Biochem (Tianjin, China). N-(2-butyl-1,3-dioxo-2,3-dihydro-1H-phenalen-6-yl)-2-chloroacetamide (NCEN) and 3-O-p-ethylbenzoylflavone (3-EBF) were synthesized according to the previously reported literatures [25,26]. Butyrylthiocholineiodide (BTch) and galanthamine hydrobromide were purchased from TCI (Shanghai, China). Z-Gly-Gly-Arg-AMC acetate (Z-GGRAMC acetate) was purchased from Med Chem Express CO., Ltd. (Shanghai, China). Thrombin (Lot No. F1700752P2) was obtained from Hyphen BioMed. (France). Pooled human plasma samples were obtained from healthy donors (16 individual Mongolian including 8 males and 8 females, 20–38 years old). Ethical approval was given by the medical ethics committee of The First Affiliated Hospital of Dalian Medical University (Dalian, China), with the reference number of LCKY2015–12 approved on June 2015. Pooled human liver microsomes (HLMs, from 50 donors, lot no. X008067), Recombinant CES1A (Batch No.150006A), CES2A (Batch No.153015A) and Pooled human intestinal microsomes (HIMs, lot no. X02801) were obtained from Bioreclamation IVT (Baltimore, MD, USA) and the ethics policy statements and the product report have been added in supplementary information. Each tested compound was dissolved in dimethyl sulfoxide (LC grade, Tedia, USA) at 4 °C until use. Phosphate buffered saline (0.1 M, pH 7.4), ultrapure water from Millipore water system and LC grade acetonitrile (Tedia, USA) were used for all experiments. Cell culture medium and fetal bovine serum were acquired from Hylcone (Logan, UK). HepG2 cell was purchased from the American Type Culture Collection (Teddington, Middlesex, UK) and the validation of HepG2 cells gene test report has been shown in supplementary information.

2.2. Inhibition assays

2.2.1. General procedure of CES2A inhibition assays using FD, 3-EBF or NCEN as substrate

In this study, three known fluorogenic substrates for CES2A, including FD, 3-EBF and NCEN were used for CES2A inhibition assays [25–27]. The procedure for screening of CES2A inhibitors using these three fluorogenic substrates have been reported in some literatures [20,24,25]. The chemical structures and detection conditions of the hydrolytic metabolites of these fluorogenic substrates have been listed in Table S2. The fluorescent signals of the hydrolytic metabolite of these fluorogenic substrates were recorded by a multi-Mode microplate reader (SpectraMax® iD3, Molecular Devices, Austria).

2.2.2. General procedure of CES2A inhibition assay using irinotecan as substrate

Irinotecan, a known CES2A substrate-drug, was also used to ascertain whether the identified CES2A inhibitor(s) displayed strong inhibition on CES2A-mediated irinotecan hydrolysis [24]. In brief, a mixture (0.2 ml) containing PBS buffer (0.1 M, pH 7.4), HLM and HIM (200 μg/ml) and varying concentrations of glabridin were pre-incubated at 37 °C for 3 min. After that, irinotecan (5 μM, final concentration) was added to start the biotransformation. Following 60 min incubation, the hydrolytic reaction was stopped by adding ice-cold acetonitrile (0.2 ml). The sample was then centrifuged to take the supernatant for quantitative analysis. The detection conditions of irinotecan and its hydrolytic metabolite SN-38 were depicted previously [28].

2.2.3. General procedure of CES1A inhibition assay using DME as substrate

DME, a bioluminogenic probe substrate for human carboxylesterase 1 (CES1A), was used for sensing the residual activities of CES1A with or without inhibitors [29]. The procedure for CES1A inhibition assay using DME as a probe substrate has been reported previously [24]. In brief, a mixture reaction system (0.1 ml) including HLM and each test compound was firstly pre-incubated for 3 min at 37 °C and then DME was added to initiate the hydrolytic reaction. After 10 min incubation, equal volume of LDR was added to stop reaction. The chemical structures of DME and its hydrolytic metabolite (D-luciferin), as well as their detection conditions were depicted in Table S2.

2.2.4. General procedure of AADAC inhibition assay using phenacetin as substrate

Phenacetin, a known AADAC substrate-drug, was used for sensing the residual activities of human AADAC in the presence of identified CES2A inhibitor. The incubation mixture (0.2 ml) for AADAC inhibition assay included 0.1 M buffer PBS, HLM and each test compound. Pre-incubated for 3 min at 37 °C and then phenacetin was added to initiate the hydrolytic reaction. The hydrolytic reaction was terminated by the addition of ice-cold acetonitrile (0.2 ml). The mixture was then kept on ice until centrifugation at 20,000 *g* for 20 min at 4 °C. The supernatant was then used for LC-MS/MS analysis. The detection conditions of phenacetin and its hydrolytic metabolite have been reported previously [24].

2.2.5. General procedure of BuChE inhibition assay using BTch as substrate

BTch, a known substrate for BuChE, was used for sensing the real activities of BuChE by a classic Ellman's method [30]. In this study, human plasma and purified BuChE (2 μl, 4 U/ml) from human plasma were used as enzyme source, while galanthamine hydrobromide was used as a positive control of BuChE.Human plasma was diluted 50 times prior to incubation, while the final concentration of BTch was 300 μM (near the K_m value for hydrolysis of BuChE in human plasma). Initial increasing rates of OD values of its hydrolytic metabolite formation (V_{od}, 1/min) were further analyzed by Molecular Devices that has been described as above mentioned. The absorption wavelength of OD values was set at 412 nm.

2.2.6. General procedure of thrombin inhibition assay using Z-GGRAMC as substrate

Z-GGRAMC was used as a probe substrate for sensing the hydrolytic activity of thrombin according to a previously reported method with minor modification [31]. In brief, an incubation mixture consisted of the enzyme (human thrombin with the final concentration of 0.1 NIH/ml), Tris buffer, NaCl, BSA, and each inhibitor at different concentrations. Following pre-incubation at 37 °C for 3 min, the reaction was started by the addition of *Z*-GGRAMC acetate. The chemical structures of Z-GGRAMC and its hydrolytic metabolite, as well as the detection conditions were also depicted in Table S2.

2.2.7. General procedure of DPP-4 inhibition assay using GP-BAN as substrate

GP-BAN, a newly reported highly specific fluorogenic probe for DPP-4, was used as a probe substrate for sensing the residual activities of DPP-4 with or without inhibitors. Briefly, an incubation mixture consisted of human plasma (20-time dilution), 0.1 M buffer PBS, HLM and each test compound at different concentrations. After pre-incubated for 3 min, the reaction was started by the addition of GP-BAN (100 μM, final concentration). The detection conditions of GP-BAN and its hydrolytic metabolite were depicted previously [32].

2.3. Inhibition kinetic analyses

In this study, a panel of inhibition kinetic analyses were conducted to determine the K_i values and to investigate the inhibition mode of glabridin against CES2A-mediated hydrolysis of various substrates. To this end, set of analyses that use varying concentrations of each CES2A substrate and a series of concentrations of glabridin were conducted and the results were carefully analyzed. The K_i values and inhibition mode were determined by fitting the kinetic data to a competitive, non-competitive, uncompetitive, or mixed inhibition model by nonlinear regression analysis using GraphPad Prism 7.0, as described in some previous reports [24,33–35].

2.4. Cell culture and fluorescence imaging analysis

The HepG2 cells were cultured in MEM medium supplemented with 10% fetal bovine serum, 100 U/ml penicillin and 100 μg/ml streptomycin. Cells were seeded in quadruplicate on 96-well plates and incubated overnight to ensure cell adhesion. The cells were then treated with a series of concentrations of glabridin and incubated for 30 min at 37 °C under 5% CO_2. To measure the function of intracellular CES2A, HepG2 cells were treated for 50 min with 1 μM Hoechst 33342, 10 μM NCEN, washed, and then analyzed by using an ImageXpress® Micro Confocal High-Content Imaging system (BioTek, USA).

2.5. Molecular dynamics simulations

The modelling structure of CES2A was depicted previously [36]. Gromacs (version 2016.5) was used to perform all molecular dynamics simulations [37]. The CHARMM36 all-atom force field parameters were used for proteins [38]. The force field parameters of glabridin was generated by the CHARMM General Force Field (CGenFF) [39]. All the systems were solved in a TIP3P water box and counterions were added [40]. The simulation parameters setting was depicted previously [41–45]. The simulations were performed with NPT ensemble. Trajectory analyses and visualization of structures were performed using PyMOL v2.3 (Schrodinger, LLC) and Discovery Studio Visualizer v19.1 (Dassault Systèmes Biovia Corp). The total deviation of atoms was analyzed by the root-mean-square deviation (RMSD). The RMSD of ligand was analyzed align to their initial docking structure after the least square fit of protein backbone. The online server Computed Atlas of Surface Topography of proteins (CASTp) was used to compare the solute accessible pocket volumes of catalytic-site bound protein and *Z*-site bound protein [46]. The SA pocket volumes of proteins were calculated using the probe with the radius of 2 Å after removing the ligands.

2.6. Statistical analysis

All experiments in this study were conducted at least three times. The IC_{50} values and K_i values were calculated using GraphPad Prism 7.0 software (GraphPad Software, Inc., La Jolla, USA).

3. Results

3.1. Screening of selective CES2A inhibitors from natural product library

To find a potent and specific CES2A inhibitor, more than hundreds of natural compounds were collected and their inhibitory potentials on human carboxylesterases (including CES1A and CES2A) were assayed. As shown in **Table S1**, most of compounds displayed relative weak inhibition on CES1A in contrast to the positive CES1A inhibitor (oleanolic acid, OA). By contrast, CES2A could be inhibited by many natural compounds. Among all tested compounds, glabridin (a bioactive compound of *Glycyrrhiza glabra* L.) displayed the most efficacious inhibition capability towards CES2A-mediated FD hydrolysis in HLM (IC_{50} = 0.15 μM) as well as high specificity over CES1A (>500-fold). Meanwhile, the inhibition potential of LPA (a known CES2A inhibitor) against CES2A-mediated FD hydrolysis in HLM was also assayed under some conditions, and the IC_{50} value of LPA was determined as 6.47 μM, which was 43-fold of that glabridin. These findings suggested that

Table 1
The inhibition parameters and inhibition modes of glabridin against CES2A-mediated hydrolysis of various substrate.

Target enzyme	Enzyme source	Microsomal protein concentration (μg/ml)	Substrate	IC_{50} (μM)	f_u	K_i (μM)	$f_u{}^*K_i$ (μM)	Inhibition mode	Goodness of fit (R^2)
CES2A	HLM	2	FD	0.15 ± 0.02	0.96	0.27	0.26	Mixed	0.99
CES2A	HLM	10	3-EBF	0.31 ± 0.02	0.83	0.34	0.28	Mixed	0.99
CES2A	HLM	10	NCEN	1.09 ± 0.08	0.83	0.60	0.50	Mixed	0.99
CES2A	HLM	200	CPT-11	10.91 ± 1.92	0.20	15.17	3.03	Mixed	0.99

Note: Estimate the *in vitro* fraction unbound from drug's properties. Equations published by Austin are being used for this calculation. For microsomes: % unbound = 100/[MicrosConc * [10^[0.56 * logD/P-1.41]] + 1] [47]; logP value of glabridin was set to 4.8.

glabridin was a potent and specific CES2A inhibitor, which prompted us to deepen and extend our investigation on the specificity and inhibition mechanism of glabridin on this enzyme.

3.2. Specificity of glabridin on CES2A over other human serine hydrolases

In view of that the inhibitor spectra of mammalian serine hydrolases are highly overlapped, it is necessary to investigate the specificity of glabridin on CES2A over other human serine hydrolases, especially for those enzymes participating in endogenous metabolism. As depicted in Table S1, the IC_{50} value of glabridin towards CES1A-meadiated DME hydrolysis in HLM was evaluated as 81.83 μM, which was over 500-fold larger than that on CES2A. To further confirm the specificity of glabridin towards CES2A over other human serine hydrolases, the inhibitory effects of glabridin on the catalytic activity of four abundant human serine hydrolases (including AADAC, BuChE, thrombin and DPP-4) were determined, and the result showed that glabridin was hardly inhibit these serine hydrolases, with the IC_{50} values of >100 μM (Table S3). To further confirm the specificity of glabridin towards CES2A over CES1A, we used recombinant human CES2A and CES1A as enzyme sources. The results demonstrated that the IC_{50} value of glabridin against CES2A-mediated FD hydrolysis in recombinant CES2A was 0.08 μM, while the IC_{50} of glabridin against CES1A-mediated DME hydrolysis in recombinant CES1A was 71.24 μM (Fig. S6). This finding clearly demonstrated that glabridin was a specific inhibitor against CES2A over CES1A. Meanwhile, the inhibition potential of glabridin against BuChE was also assayed using purified BuChE as enzyme source, the result showed that glabridin was hardly inhibit BuChE, with the IC_{50} values of >100 μM (Fig. S7). These results clearly demonstrated that glabridin was a highly specific CES2A inhibitor over other serine hydrolases in the human body, implying that this natural compound might not disturb endogenous metabolism *via* inhibiting some key serine hydrolases participating in endogenous metabolism.

3.3. Inhibition of CES2A-mediated hydrolysis of different substrates by glabridin

Prior to inhibition kinetic analyses, we compared the IC_{50} values of glabridin against CES2A-mediated FD hydrolysis with different pre-incubation times (3 min and 33 min). As depicted in Fig. S2, the inhibition curves and the IC_{50} values were very closed to each other, suggesting that glabridin was not a time-dependent inhibitor but a reversible inhibitor of CES2A. Considering that CES2A had multiple different ligand-binding sites, it was necessary to investigate the inhibition behaviors of glabridin on CES2A using various CES2A substrates. Thus, in this study, four optical CES2A substrates (FD, 3-EBF, NCEN and irinotecan) with different binding sites on CES2A were used. As listed in Table 1 and Fig. 2, glabridin could strongly inhibited CES2A-

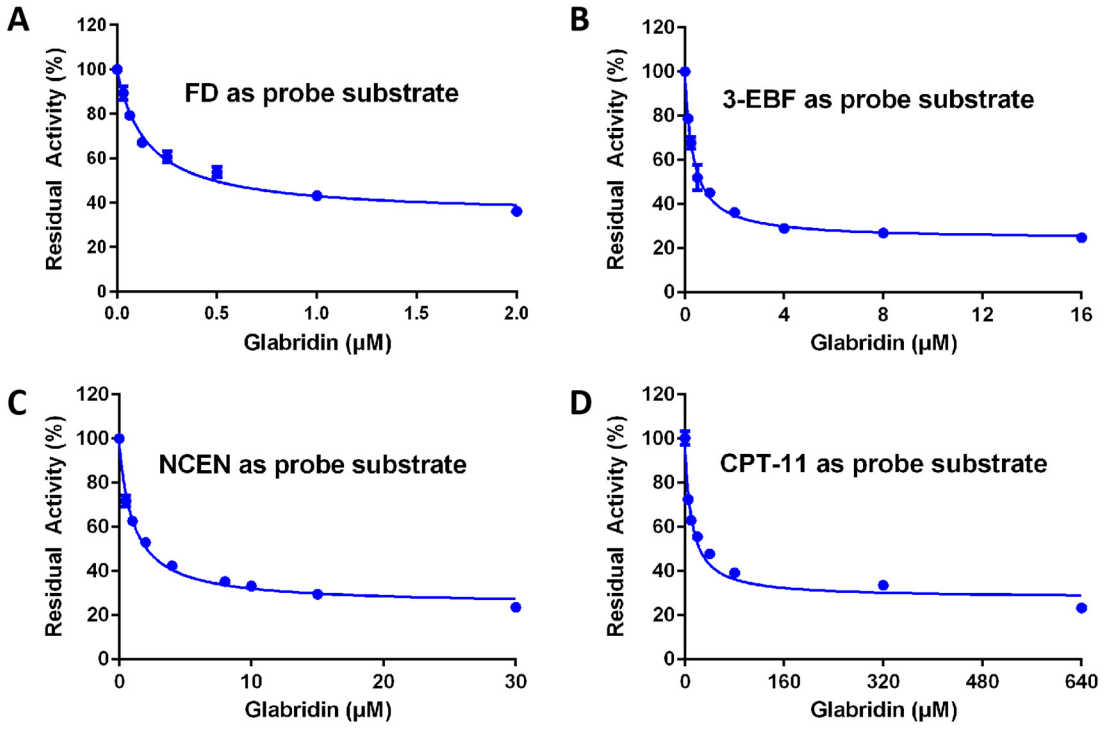

Fig. 2. The dose-response inhibition curves of glabridin on CES2A using FD (A), 3-EBF (B), NCEN (C) and CPT-11 (D) as probe substrate, respectively. All data were shown as mean ± SD of triplicate determinations.

mediated FD, 3-EBF and NCEN hydrolysis in HLM, with the IC_{50} values of 0.15 μM, 0.31 μM, and 1.09 μM, respectively. The apparent IC_{50} value of glabridin on CES2A-mediated irinotecan hydrolysis in HLM was also determined as 10.91 μM (Table 1), which is much higher than that of glabridin on CES2A-mediated hydrolysis of other substrates. The higher IC_{50} value of glabridin on CES2A-mediated irinotecan hydrolysis in HLM can be attributed to the high final concentration of microsomal protein for catalyzing irinotecan hydrolysis [47]. Furthermore, the inhibitory effect of glabridin on CES2A-mediated irinotecan hydrolysis was also investigated in HIM. As listed in Fig. S8, glabridin could strongly inhibited CES2A-mediated irinotecan hydrolysis in HIM, with the apparent IC_{50} value of 6.91 μM.

Next, the inhibition kinetics of glabridin against CES2A-mediated hydrolysis of different substrates were carefully investigated. The Lineweaver-Burk plots suggested that glabridin inhibited CES2A-mediated FD, 3-EBF, NCEN and irinotecan hydrolysis *via* a mixed manner (Fig. 3), with the K_i values of 0.27 μM, 0.34 μM, 0.60 μM, 15.17 μM, respectively (Table 1). To precisely character the inhibition potentials of glabridin, we correct these K_i values using the unbound fraction of

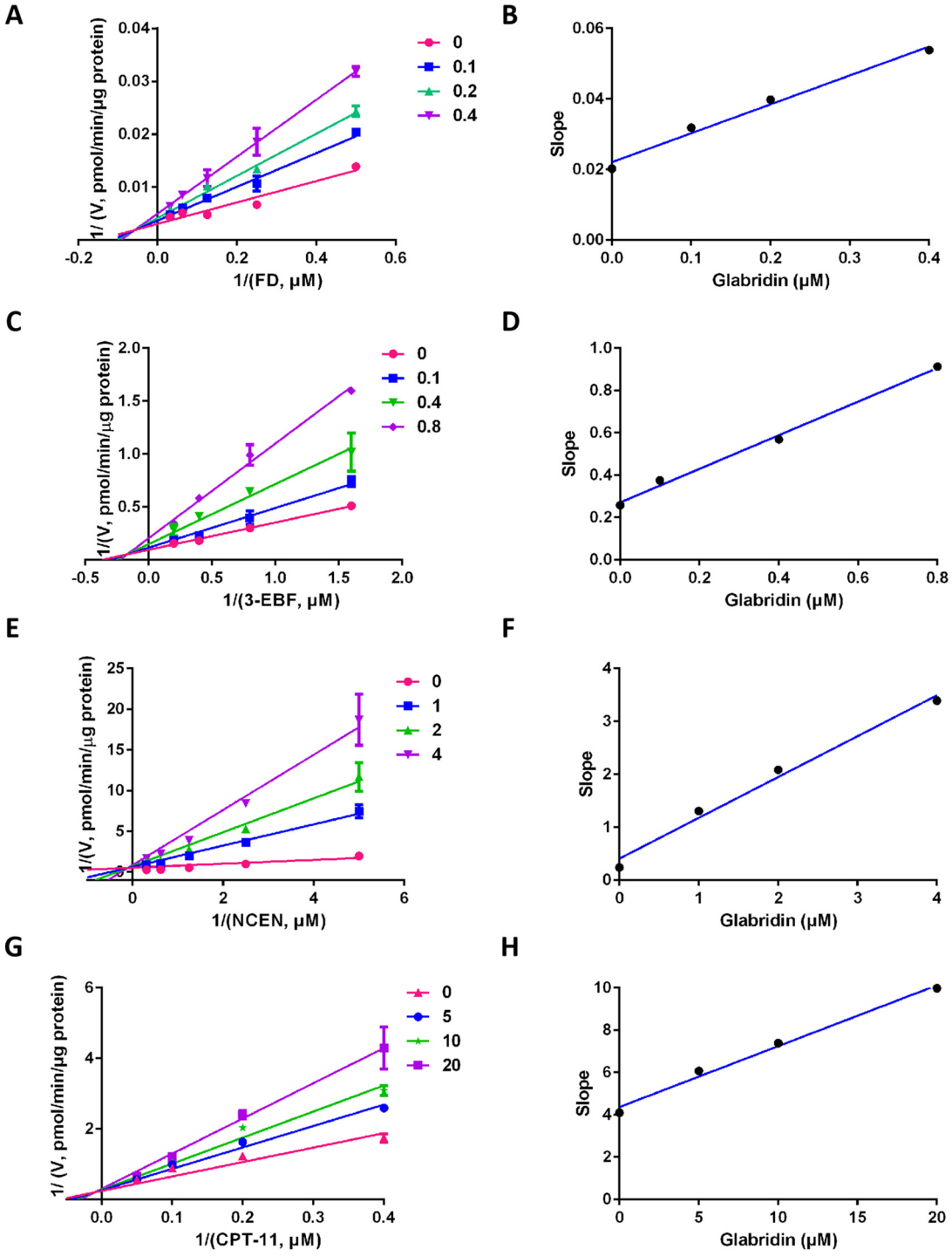

Fig. 3. The Lineweave-Burk plots of glabridin against CES2A-mediated FD (A), 3-EBF (C), NCEN (E) and CPT-11 (G) hydrolysis, and the second plots of slopes from the Lineweaver-Burk plot for glabridin inhibition on CES2A-mediated FD (B), 3-EBF (D), NCEN (F) and CPT-11 (H) hydrolysis. All data were shown as mean ± SD of triplicate assays.

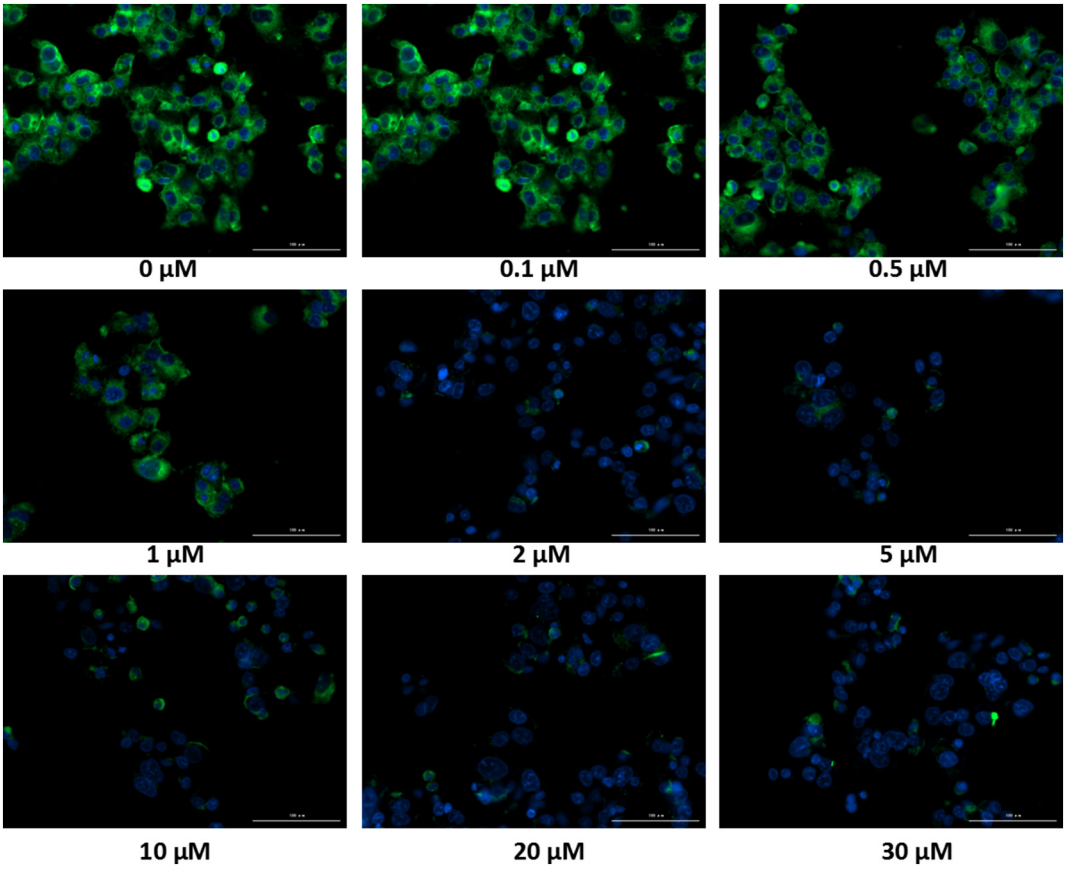

Fig. 4. The images of HepG2 cells stained with NCEN (10 μM) and Hoechst 33342 (1 μM) at 37 °C for 50 min upon addition of glabridin at various concentrations (0 μM, 0.1 μM, 0.5 μM, 1 μM, 2 μM, 5 μM, 10 μM, 20 μM and 30 μM).

inhibitor concentration (*fu*) [48,49]. As shown in Table 1, the fu^*K_i values of glabridin against CES2A-meidated FD, 3-EBF, NCEN and irinotecan hydrolysis were determined as 0.26 μM, 0.28 μM, 0.50 μM and 3.03 μM, respectively. These results demonstrated that glabridin was capable of inhibiting CES2A-mediated hydrolysis of a panel of substrates, including irinotecan.

3.4. Inhibition of CES2A by glabridin in living HepG2 cells

In view of that CES2A is an intracellular enzyme, it is necessary to investigate the inhibition potential of glabridin on intracellular CES2A in living cells. To this end, NCEN was used as a practical florescent substrate for sensing residual CES2A activities in living cells due to its excellent optical properties [25], while HepG2 cells was used for this assay. Prior to the studies on living cells, the cytotoxicity of glabridin on living HepG2 cells was assays. As shown in Fig. S3, glabridin was hardly affect HepG2 cell's viability when its concentration was lower than 40 μM. In this case, the following assays in living HepG2 cells was proceeded with a series of glabridin concentrations <40 μM. As shown in Fig. 4, upon addition of glabridin, the green fluorescence signals of NAH (the hydrolytic metabolite of NCEN) in living HepG2 cells could be remarkably reduced *via* a dose-dependent manner, suggesting the CES2A activities in living HepG2 cells were strongly blocked by glabridin. Notably, the IC_{50} value of glabridin against intracellular CES2A in living HepG2 cells was determined as low as 0.52 μM, which was much lower than other reported CES2A inhibitors [18,20]. These results demonstrated that glabridin was cell permeable and capable of inhibiting intracellular CES2A with a very low IC_{50} value.

3.5. Molecular dynamics simulation of CES2A

It is well-known that molecular dynamics simulations could provide the dynamical and structural information of protein-ligand interactions. In this study, to get microscopic insights into the inhibition mechanism of glabridin against CES2A, molecular dynamics simulations were performed. As shown in Fig. 5, following 15 ns simulation, the glabridin-

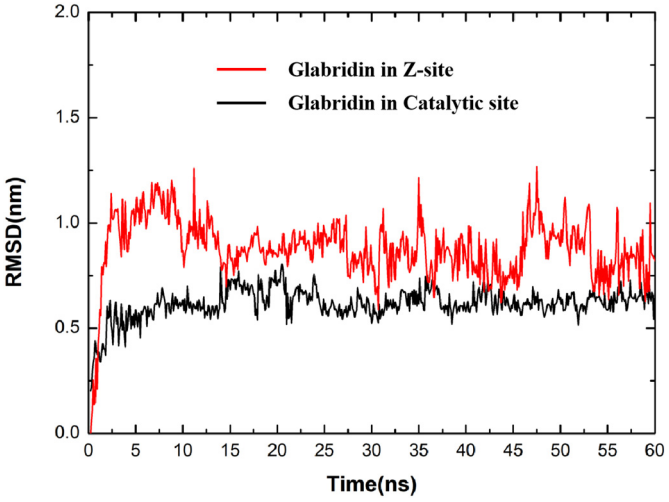

Fig. 5. The RMSD fluctuation of glabridin in the catalytic cavity (black) and in the *Z*-site (red).

CES2A complex could reach dynamics equilibrium. The fluctuation of glabridin in the catalytic site within 5 Å showed high stability while that in the *Z*-site within 10 Å exhibited more flexibility. The equilibrium structure was shown in Fig. 6, it was evident that glabridin could be well-docked into two distinct ligand-binding sites of CES2A and formed stable conformation, one was located in the catalytic cavity which was highly overlapped with that of the substrate (FD) on CES2A (as a competitive inhibitor), and another one was on the regulatory domain ("Z site"), which was far away from the catalytic triad of CES2A (as a non-competitive inhibitor). The key residues for the interactions between glabridin and CES2A were also analyzed. As depicted in Fig. 6C and Fig. 6D, glabridin could interact with the surrounding residues around the catalytic cavity or the regulatory domain of CES2A mainly *via* hydrophobic interactions. Moreover, as glabridin bound on the *Z*-site, the α helix of the regulatory domain underwent a positional shift, leading a larger accessible channel of solvents (shown in Fig. S1). Upon binding of glabridin on the Z-site, the solute accessible (SA) volume was about 1168 $Å^3$ which was much larger than that binding on the catalytic site (429 $Å^3$). The exposure of the catalytic triad to the solvent may affect the hydrophobic interactions of the substrate in the catalytic pocket, and thereby slowing the turnover of this hydrolase. These results suggested that glabridin could be well-docked into both the catalytic cavity and the regulatory domain of CES2A, which provided a novel insight for understanding the interactions of glabridin and CES2A, especially for explain why glabridin functioned as a 'mixed-type inhibitor' of CES2A.

4. Discussion

Over the past decade, the tissue distribution, physiological functions, as well as substrate and inhibitor spectra of CES2A have been extensively studied [50]. As one of the most abundant esterases distributed in the human small intestine and colon, CES2A has been found with the hydrolytic activity of triacylglycerols and a wide range of xenobiotics bearing of ester or amide bonds [10–12]. Recent studies have been demonstrated that CES2A-inhibition therapy may reduce the over-accumulation of SN-38 (the cytotoxic metabolite of anticancer agent irinotecan) in the intestinal tract, and thereby ameliorate irinotecan induced life-threatening diarrhea in those patients receiving irinotecan, which will be very helpful for improving the patient's quality of life. With this goal in mind, many researchers are committed to discover more CES2A inhibitors with high specificity and improved properties. Until now, hundreds of CES2A inhibitors with various scaffolds have been reported and most of them have been well-summarized in several newly published reviews [19,21], but the efficacious and selective CES2A inhibitors that are capable of targeting intracellular CES2A have been rarely reported. Thus, it is urgent to find more efficacious CES2A inhibitors with high specificity and good cell permeability as ideal lead compound(s) for the development of druggable CES2A inhibitors that have improve safety profiles and the capability of targeting intracellular CES2A.

In this study, a large-scale screening campaign was performed for discovery of a potent and specific CES2A inhibitors from natural

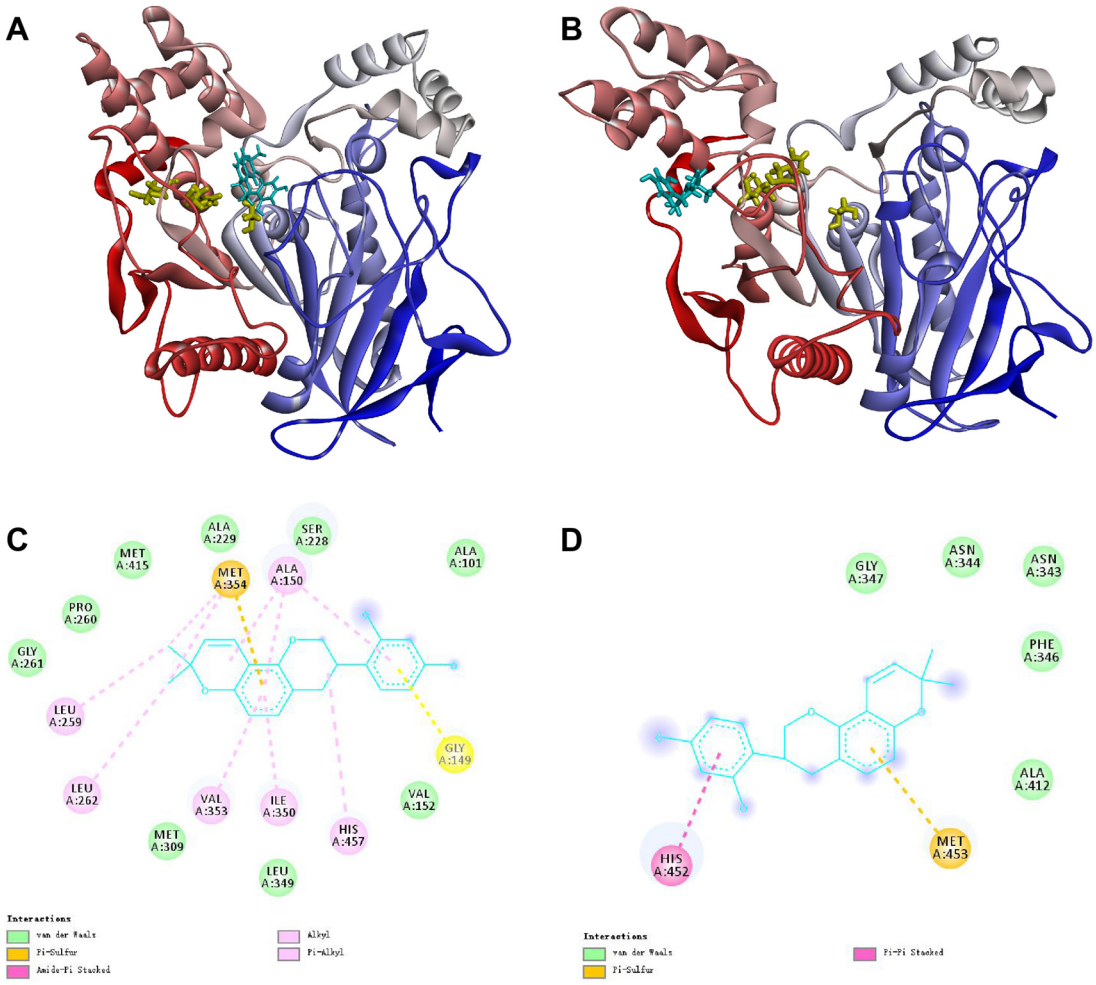

Fig. 6. The stereodiagram of glabridin equilibrium in the active site (A) or the Z-site (B) of CES2A. The detailed interactions between glabridin and the amino acid residues in the area surrounding to the active site (C) and Z-site (D) of CES2A. Note that the catalytic triad of CES2A (Ser^{228}, Glu^{345} and His^{457}) are shown as yellow sticks, while the glabridin is shown as blue sticks.

products, by considering that natural products were the main sources of new drug research and development [51]. To this end, a panel of fluorescence-based biochemical assays was constructed for high-throughput screening of the inhibition potentials of each compounds on CES2A and other key serine hydrolases that participates in a variety of physiological processes in the human body [52]. Following screening of more than one hundred of natural products, glabridin (a bioactive compound of *Glycyrrhiza glabra* L.) was found with potent CES2A inhibition activity (IC_{50} = 0.15 μM) and high specificity over CES1A (>500-fold) and other key serine hydrolases in the human body, such as BuChE, DPP-4 and thrombin. Notably, the potency of glabridin against CES2A was 43-fold better than that of LPA (a clinically used specific CES2A inhibitor), suggesting that glabridin hold a great potential to replace LPA as a potent inhibitor for CES2A-inhibition therapy. More importantly, the capability of glabridin targeting intracellular CES2A was also carefully investigated using NCEN as a practical florescent substrate for sensing the residual CES2A activities in living cells. The results showed that glabridin was a cell permeable and low cytotoxic agent, this natural compound displayed relatively low cytotoxicity and potent inhibitory effect on intracellular CES2A in living HepG2 cells, with the IC_{50} value of 0.52 μM. To the best of our knowledge, the potency of glabridin targeting intracellular CES2A was much better than other reported CES2A inhibitors [18,20].

In addition to the CES2A inhibition activity, glabridin has been found with a variety pharmacological activities, including anti-oxidation, anti-inflammatory, anti-atherosclerosis, anti-bacterial, and anti-tumor activity [23]. These beneficial effects are very helpful for ameliorating the oxidative damage of intestinal epithelial cells and the inflammatory progression in patients with the intestinal toxicity caused by irinotecan [53]. Although glabridin is not a marketed drug now, licorice flavonoids oil (LFO), a commercially available dietary product that contains ~2.90% glabridin, has been widely used for the treatment of overweight and obesity [54]. Recent studies have found that LFO displayed many beneficial effects, such as anti-obesity, hypoglycemic and antioxidant effects [55]. Clinical studies have suggested that LFO is a very safe product, and no clinically significant adverse events occurred when it is given to healthy or overweight subjects for up to 12 weeks [54]. A preclinical toxicological study has also reported that the no-observed adverse effect level for LFO is estimated to be 800 mg/kg/day for female rats [56]. As an edible herb product, the recommended oral dosage of LFO is up to 1200 mg/d [57], which means that the daily dosage of glabridin will be up to 34.8 mg/d. Considering that the total volume of the human gastrointestinal system in adults is 4 L and the molecular weight of glabridin is 324.37 Da, the local exposure of glabridin in the gastrointestinal system will be up to 26.8 μM. Such exposure is much higher than the IC_{50} value of glabridin on intracellular CES2A. It has also been reported that glabridin can be easily absorbed into the intestinal cells and released to the basolateral side as the free aglycone form rather than its conjugated forms [58], but this natural compound can be readily *O*-glucuronidated by hepatic UDP-glucuronosyltransferases [59]. Such pharmacokinetic features suggest that the local exposure of glabridin in the gastrointestinal system will be much higher than that in plasma and liver, which may avoid disturbing the functions of other organ or systems. These accumulative evidences indicate that glabridin-containing dietary product LFO has good safety profiles, and this dietary product may be a good choice for ameliorating irinotecan trigger life-threatening diarrhea in clinic.

From the viewpoint of medicinal chemistry, glabridin has two phenolic groups at the C-2′ and C-4′ sites which can be easily modified to generate a range of derivatives with good structural connectivity (Fig. 1). Notably, the scheme for total synthesis of glabridin has been reported [60], which means that the chemists can readily get glabridin and its derivatives for further pharmacological and toxicological studies. Considering that the predominant interactions between glabridin and CES2A are hydrophobic interactions, two phenolic groups at the C-2′ and C-4′ sites can be modified by some hydrophobic substitutes. In the future, it is necessary to synthesize a variety of structurally diverse glabridin derivatives for the studies on structure-activity relationships of these derivatives as CES2A inhibitors. Furthermore, computer aided design and virtual screening techniques should be used to modify these glabridin derivatives for simultaneous optimization of their inhibition potency and specificity, as well as the druglikeness properties.

5. Conclusion

In summary, a potent and highly specific CES2A inhibitor was found and full-characterized in this study. Following screening of more than one hundred of natural products, glabridin (a bioactive compound of *Glycyrrhiza glabra* L.) was found with potent CES2A inhibition activity (IC_{50} = 0.15 μM) and high specificity over CES1A (>500-fold) and other human serine hydrolases. A panel of inhibition kinetic analyses demonstrated that glabridin could strongly inhibit CES2A-mediated hydrolysis of various substrates *via* a mixed manner, with the $f_u{}^*K_i$ values ranged from 0.26 μM to 3.03 μM. Further investigation showed that glabridin was a cell permeable and low cytotoxic agent, and this natural compound displayed potent inhibitory effects on intracellular CES2A in living HepG2 cells with the IC_{50} value of 0.52 μM. Additionally, molecular dynamics simulations suggested that glabridin could be well-docked into both the catalytic cavity and the regulatory domain of CES2A and formed relatively stable conformation, which agreed well with the mixed inhibition mode of glabridin towards CES2A, also provided a novel insight for deeper understanding the interactions of glabridin and CES2A. These findings suggested glabridin was an ideal lead compound for the development of new generation of specific CES2A inhibitors targeting intracellular CES2A, which might provide a new therapeutic alternative for alleviating irinotecan-induced diarrhea or for modulating the pharmacokinetic behaviors of CES2A-substrate drugs.

Declaration of Competing Interest

The authors have no conflicts of interests.

Acknowledgments

This work was supported by the National Key Research and Development Program of China (2017YFC1700200, 2017YFC1702000), the NSF of China (81703604, 81773687, 81803489, 81672961 and 81573501), Program of Shanghai Academic/Technology Research Leader (18XD1403600), Shuguang Program (No. 18SG40) supported by Shanghai Education Development Foundation and Shanghai Municipal Education Commission, the Innovative Entrepreneurship Program of High-level Talents in Dalian (2017RQ121 & 2016RQ025), National Undergraduate Training Program for Innovation and Entrepreneurship (No. 201710141980301090 4) and Undergraduate Training Program for Innovation and Entrepreneurship from Shanghai University of Traditional Chinese Medicine, National Engineering Research Center for Gelatin-based Traditional Chinese Medicine.

Appendix A. Supplementary data

Supplementary data to this article can be found online at https://doi.org/10.1016/j.ijbiomac.2019.06.235.

References

[1] S.P. Sanghani, P.C. Sanghani, M.A. Schiel, W.F. Bosron, Human carboxylesterases: an update on CES1, CES2 and CES3, Protein Pept. Lett. 16 (2009) 1207–1214.
[2] T. Satoh, M. Hosokawa, Structure, function and regulation of carboxylesterases, Chem. Biol. Interact. 162 (2006) 195–211.
[3] M. Hosokawa, Structure and catalytic properties of carboxylesterase isozymes involved in metabolic activation of prodrugs, Molecules 13 (2008) 412–431.
[4] T. Imai, Human carboxylesterase isozymes: catalytic properties and rational drug design, Drug Metab. Pharmacokinet. 21 (2006) 173–185.

[5] A.D. Quiroga, L. Li, M. Trötzmüller, R. Nelson, S.D. Proctor, H. Köfeler, R. Lehner, Deficiency of carboxylesterase 1/esterase-x results in obesity, hepatic steatosis, and hyperlipidemia, Hepatology 56 (2012) 2188–2198.
[6] S. Nagashima, H. Yagyu, N. Takahashi, T. Kurashina, M. Takahashi, T. Tsuchita, F. Tazoe, X.L. Wang, T. Bayasgalan, N. Sato, K. Okada, S. Nagasaka, T. Gotoh, M. Kojima, M. Hyodo, H. Horie, Y. Hosoya, M. Okada, Y. Yasuda, H. Fujiwara, M. Ohwada, S. Iwamoto, M. Suzuki, H. Nagai, S. Ishibashi, Depot-specific expression of lipolytic genes in human adipose tissues-association among CES1 expression, triglyceride lipase activity and adiposity, J. Atheroscler. Thromb. 18 (2011) 190–199.
[7] P.M. Potter, J.S. Wolverton, C.L. Morton, M. Wierdl, M.K. Danks, Cellular localization domains of a rabbit and a human carboxylesterase: influence on irinotecan (CPT-11) metabolism by the rabbit enzyme, Cancer Res. 58 (1998) 3627–3632.
[8] S.K. Quinney, S.P. Sanghani, W.I. Davis, T.D. Hurley, Z. Sun, D.J. Murry, W.F. Bosron, Hydrolysis of capecitabine to 5′-deoxy-5-fluorocytidine by human carboxylesterases and inhibition by loperamide, J. Pharmacol. Exp. Ther. 313 (2005) 1011–1016.
[9] T. Fukami, M. Kariya, T. Kurokawa, A. Iida, M. Nakajima, Comparison of substrate specificity among human arylacetamide deacetylase and carboxylesterases, Eur. J. Pharm. Sci. 78 (2015) 47–53.
[10] J. Lian, R. Nelson, R. Lehner, Carboxylesterases in lipid metabolism: from mouse to human, Protein Cell 9 (2018) 178–195.
[11] S. C. Laizure, R. B. Parker, V. L. Herring, L. Vanessa, Z. Y. Hu, Identification of carboxylesterase-dependent dabigatran etexilate hydrolysis, Drug Metab. Dispos. 42 (2014) 201–206.
[12] R. Humerickhouse, K. Lohrbach, L. Li, W.F. Bosron, M.E. Dolan, Characterization of CPT-11 hydrolysis by human liver carboxylesterase isoforms hCE-1 and hCE-2, Cancer Res. 60 (2000) 1189–1192.
[13] U. Swami, S. Goel, S. Mani, Therapeutic targeting of CPT-11 induced diarrhea: a case for prophylaxis, Curr. Drug Targets 14 (2013) 777–797.
[14] M.K. Ma, H.L. McLeod, Lessons learned from the irinotecan metabolic pathway, Curr. Med. Chem. 10 (2003) 41–49.
[15] X.X. Yang, Z.P. Hu, S.Y. Chan, E. Chan, B.C. Goh, W. Duan, S.F. Zhou, Novel agents that potentially inhibit irinotecan-induced diarrhea, Curr. Med. Chem. 12 (2005) 1343–1358.
[16] P.J. Tobin, H.M. Dodds, S. Clarke, M. Schnitzler, L.P. Rivory, The relative contributions of carboxylesterase and beta-glucuronidase in the formation of SN-38 in human colorectal tumours, Oncol. Rep. 10 (2003) 1977–1979.
[17] L.D. Hicks, J.L. Hyatt, S. Stoddard, L. Tsurkan, C.C. Edwards, R.M. Wadkins, P.M. Potter, Improved, selective, human intestinal carboxylesterase inhibitors designed to modulate 7-ethyl-10-[4-(1-piperidino)-1-piperidino]carbonyloxycamptothecin (Irinotecan; CPT-11) toxicity, J. Med. Chem. 52 (2009) 3742–3752.
[18] L.W. Zou, Y.G. Li, P. Wang, K. Zhou, J. Hou, Q. Jin, Design, synthesis, and structure-activity relationship study of glycyrrhetinic acid derivatives as potent and selective inhibitors against human carboxylesterase 2, Eur. J. Med. Chem. 112 (2016) 280–288.
[19] L.W. Zou, Q. Jin, D.D. Wang, Q.K. Qian, D.C. Hao, G.B. Ge, L. Yang, Carboxylesterase inhibitors: an update, Curr. Med. Chem. 25 (2018) 1627–1649.
[20] Z.M. Weng, G.B. Ge, T.Y. Dou, P. Wang, P.K. Liu, X.H. Tian, N. Qiao, Y. Yu, L.W. Zou, Q. Zhou, W.D. Zhang, J. Hou, Characterization and structure-activity relationship studies of flavonoids as inhibitors against human carboxylesterase 2, Bioorg. Chem. 77 (2018) 320–329.
[21] D.D. Wang, L.W. Zou, Q. Jin, J. Hou, G.B. Ge, L. Yang, Recent progress in the discovery of natural inhibitors against human carboxylesterases, Fitoterapia 117 (2017) 84–95.
[22] H. Miller, L. Panahi, D. Tapia, A. Tran, J.D. Bowman, Loperamide misuse and abuse, J. Am. Pharm. Assoc. 57 (2003) 45–50.
[23] C. Simmler, G.F. Pauli, S.N. Chen, Phytochemistry and biological properties of glabridin, Fitoterapia 90 (2013) 160–184.
[24] Y.Q. Wang, Z.M. Weng, T.Y. Dou, J. Hou, D.D. Wang, L.L. Ding, L.W. Zou, Y. Yu, J. Chen, H. Tang, G.B. Ge, Nevadensin is a naturally occurring selective inhibitor of human carboxylesterase 1, Int. J. Biol. Macromol. 120 (2018) 1944–1954.
[25] Q. Jin, L. Feng, D.D. Wang, Z.R. Dai, P. Wang, L.W. Zou, Z.H. Liu, J.Y. Wang, Y. Yu, G.B. Ge, J.N. Cui, L. Yang, A two-photon ratiometric fluorescent probe for imaging carboxylesterase 2 in living cells and tissues, ACS Appl. Mater. Interfaces 7 (2015) 24874–24881.
[26] L. Feng, Z.M. Liu, J. Hou, X. Lv, J. Ning, G.B. Ge, J.N. Cui, L. Yang, A highly selective fluorescent ESIPT probe for the detection of human carboxylesterase 2 and its biological applications, Biosens. Bioelectron. 65 (2015) 9–15.
[27] J. Wang, E.T. Williams, J. Bourgea, Y.N. Wong, C.J. Patten, Characterization of recombinant human carboxylesterases: fluorescein diacetate as a probe substrate for human carboxylesterase 2, Drug Metab. Dispos. 39 (2011) 1329–1333.
[28] T.F. Shao, Y.T. Zheng, J.L. Xu, W.M. Cai, An analytical method built for irinotecan and its active metabolite sn-38 in human plasma using hplc-fld, Chinese Journal of Hospital Pharmacy 32 (2012) 17–19.
[29] D.D. Wang, Q. Jin, L.W. Zou, J. Hou, X. Lv, W. Lei, A bioluminescent sensor for highly selective and sensitive detection of human carboxylesterase 1 in complex biological samples, Chem. Commun. 52 (2016) 3183–3186.
[30] G.L. Ellman, K.D. Courtney, V. Andres, R.M. Feather-Stone, A new and rapid colorimetric determination of acetylcholinesterase activity, Biochem. Pharmacol. 7 (1961) 88–95.
[31] L.H. Wei, T.R. Chen, H.B. Fang, Q. Jin, S.J. Zhang, J. Hou, Y. Yu, T.Y. Dou, Y.F. Cao, W.Z. Guo, G.B. Ge, Natural constituents of St. John's Wort inhibit the proteolytic activity of human thrombin, Int. J. Biol. Macromol. 134 (2019) 622–630.
[32] L.W. Zou, P. Wang, X.K. Qian, L. Feng, Y. Yu, D.D. Wang, Q. Jin, J. Hou, Z.H. Liu, G.B. Ge, L. Yang, A highly specific ratiometric two-photon fluorescent probe to detect dipeptidyl peptidase IV in plasma and living systems, Biosens. Bioelectron. 90 (2017) 283–289.
[33] S.L. Xiong, L.M. Yue, G.T. Lim, J.M. Yang, J. Lee, Y.D. Park, Inhibitory effect of raspberry ketone on α-glucosidase: docking simulation integrating inhibition kinetics, Int. J. Biol. Macromol. 113 (2018) 212–218.
[34] L. Gou, J. Lee, J.M. Yang, Y.D. Park, H.M. Zhou, Y. Zhan, Z.R. Lu, Inhibition of tyrosinase by fumaric acid: integration of inhibition kinetics with computational docking simulations, Int. J. Biol. Macromol. 105 (2016) 1663–1669.
[35] M. Bello, J.A. Morales-González, Molecular recognition between potential natural inhibitors of the keap1-nrf2 complex, Int. J. Biol. Macromol. 105 (2017) 981–992.
[36] A. Waterhouse, M. Bertoni, S. Bienert, G. Studer, G. Tauriello, R. Gumienny, SWISS-MODEL: homology modelling of protein structures and complexes, Nucleic Acids Res. (2018)https://doi.org/10.1093/nar/gky427.
[37] D.S.D. Van, L.E. Hess, B. Groenhof, G. Mark, A.E. Berendsen, H.J. C, GROMACS: fast, flexible, and free, J. Comput. Chem. 26 (2005) 1701–1718.
[38] K. Vanommeslaeghe, E. Hatcher, C. Acharya, S. Kundu, S. Zhong, J. Shim, E. Darian, O. Guvench, P. Lopes, I. Vorobyov, A.D. Mackerell, CHARMM general force field: a force field for drug-like molecules compatible with the CHARMM all-atom additive biological force fields, J. Comput. Chem. 31 (2010) 671–690.
[39] K. Vanommeslaeghe, A.D. MacKerell, Automation of the CHARMM General Force Field (CGenFF) I: bond perception and atom typing, J. Chem. Inf. Model. 52 (2012) 3144–3154.
[40] W.L. Jorgensen, J. Chandrasekhar, J.D. Madura, R.W. Impey, M.L. Klein, Comparison of simple potential functions for simulating liquid water, J. Chem. Phys. 79 (1983) 926.
[41] X.Q. Guan, D.Q. Wei, D. Hu, Free energy calculation of transmembrane ion permeation: sample with a single reaction coordinate and analysis along transition path, J. Chem. Theory Comput. 15 (2019) 1216–1225.
[42] T.A. Darden, D.M. York, L.G. Pedersen, Particle mesh Ewald: an N log (N) method for Ewald sums in large systems, J. Chem. Phys. 98 (1992) 10089–10092.
[43] B. Hess, H. Bekker, H.J.C. Berendsen, J.G.E.M. Fraaije, LINCS: a linear constraint solver for molecular simulations, J. Comput. Chem. 18 (1997) 1463–1472.
[44] G. Bussi, D. Donadio, M. Parrinello, G. Bussi, D. Donadio, M. Parrinello, Canonical sampling through velocity rescaling canonical sampling through velocity rescaling, J. Chem. Phys. 126 (2007), 014101.
[45] M. Parrinello, A. Rahman, Polymorphic transitions in single crystals: a new molecular dynamics method, J. Appl. Phys. 52 (1981) 7182.
[46] W. Tian, C. Chen, X. Lei, J.L. Zhao, J. Liang, CASTp 3.0: computed atlas of surface topography of proteins, Nucleic Acids Res. 46 (2018) 363–367.
[47] R.P. Austin, P. Barton, S.L. Cockroft, M.C. Wenlock, R.J. Riley, The influence of nonspecific microsomal binding on apparent intrinsic clearance, and its prediction from physicochemical properties, Drug Metab. Dispos. 30 (2002) 1497.
[48] T.D. Bjornsson, J.T. Callaghan, H.J. Einolf, V. Fischer, L. Gan, S. Grimm, J. Kao, S.P. King, G. Miwa, L. Ni, G. Kumar, J. McLeod, R.S. Obach, S. Roberts, A. Roe, A. Shah, F. Snikeris, J.T. Sullivan, D. Tweedie, J.M. Vega, J. Walsh, S.A. Wrighton, The conduct of in vitro and in vivo drug-drug interaction studies: a pharmaceutical research and manufacturers of America (PhRMA) perspective, Drug Metab. Dispos. 31 (2003) 815–832.
[49] G.T. Tucker, J.B. Houston, S.M. Huang, Optimising drug development: strategies to assess drug metabolism/transporter interaction potential-toward a consensus, Clin. Pharmacol. Ther. 70 (2001) 103–114.
[50] D.D. Wang, L.W. Zou, Q. Jin, J. Hou, G.B. Ge, L. Yang, human carboxylesterases: a comprehensive review, Acta Pharm. Sin. B 8 (2018) 699–712.
[51] D.J. Newman, G.M. Cragg, Natural products as sources of new drugs from 1981 to 2014, J. Nat. Prod. 79 (2016) 629–661.
[52] D.D. Wang, J. Ning, X. Lv, G.B. Ge, Research progress in specific probe substrates for drug metabolizing enzymes, Prog Pharm Sci 41 (2017) 110–123.
[53] H.S. Kwon, S.M. Oh, J.K. Kim, Glabridin, a functional compound of liquorice, attenuates colonic inflammation in mice with dextran sulphate sodium-induced colitis, British Society for Immunology. Clinical and Experimental Immunology. 151 (2007) 165–173.
[54] Y.J. Tominaga, K.K. Nakagawa, T. Mae, M. Kitano, S. Yokota, T. Arai, H. Ikematsu, S. Inoue, Licorice flavonoid oil reduces total body fat and visceral fat in overweight subjects: a randomized, double-blind, placebo-controlled study, Obes. Res. Clin. Pract. 3 (2009) I–IV.
[55] H. Kamisoyama, K. Honda, Y. Tominaga, S. Yokota, S. Hasegawa, Investigation of the anti-obesity action of licorice flavonoid oil in diet-induced obese rats, Biosci. Biotechnol. Biochem. 72 (2008) 3225–3231.
[56] K. Nakagawa, M. Kitano, H. Kishida, T. Hidaka, K. Nabae, M. Kawabe, K. Hosoe, 90-day repeated-dose toxicity study of licorice flavonoid oil (LFO) in rats, Food Chem. Toxicol. 46 (2008) 2349–2357.
[57] F. Aoki, K. Nakagawa, M. Kitano, H. Ikematsu, K. Nakamura, S. Yokota, Y. Tominaga, N. Arai, T. Mae, Clinical safety of licorice flavonoid oil (LFO) and pharmacokinetics of glabridin in healthy humans, J. Am. Coll. Nutr. 26 (2007) 209–218.
[58] C. Ito, N. Oi, T. Hashimoto, H. Nakabayashi, F. Aoki, Y. Tominaga, S. Yokota, K. Hosoe, K. Kanazawa, Absorption of dietary licorice isoflavan glabridin to blood circulation in rats, J. Nutr. Sci. Vitaminol. (Tokyo) 53 (2007) 358–365.
[59] B. Guo, Z.Z. Fang, L. Yang, L. Xiao, Y.L. Xia, F.J. Gonzalez, L.L. Zhu, Y.F. Cao, G.B. Ge, L. Yang, H.Z. Sun, Tissue and species differences in the glucuronidation of glabridin with UDP-glucuronosyltransferases, Chem. Biol. Interact. 231 (2015) 90–97.
[60] W.H. Ji, Q.S. Gao, Y.L. Lin, H.M. Gao, X. W., Y.L. Geng, Total synthesis of (±)-Glabridin, Synth. Commun. 44 (2014) 540–546.